Generation of Archean TTGs via Sluggish Subduction

Bradford J. Foley[1]

[1]*Department of Geosciences, Pennsylvania State University, 503 Deike Building, University Park, PA 16802*

ABSTRACT

The Trondhjemite-Tonalite-Granodiorite (TTG) suite of rocks prominent in Earth's Archean continents is thought to form by melting of hydrated basalt, but the specific tectonic settings of formation are unclear. Models for TTG genesis range from melting of downgoing mafic crust during subduction into a hotter mantle to melting at the base of a thick crustal plateau; while neither uniquely defines a global tectonic regime, the former is consistent with mobile lid tectonics and the latter a stagnant lid. One major problem for a subduction model is slabs sinking too quickly and steeply in a hotter mantle to melt downgoing crust. I show, however, that grain size reduction in the lithosphere leads to relatively strong plate boundaries on the early Earth, which slow slab sinking. During this "sluggish subduction," sinking plates can heat up enough to melt when the mantle temperature is $\gtrsim 1600^{\circ}$C. Crustal melting via sluggish subduction can thus explain TTG formation during the Archean due to elevated mantle temperatures, and the paucity of TTG production since due to mantle cooling.

1. INTRODUCTION

Earth's continents play a critical role in the evolution of the planet. Their formation redistributes elements between interior and surface (e.g., Hofmann, 1988; Rudnick & Gao, 2014) and creates exposed land upon their emergence above sea level (Flament et al., 2008; Reimink et al., 2021), influencing geochemical cycles that control atmospheric species like CO_2 (e.g., Berner et al., 1983; Hayworth & Foley, 2020) and O_2 (Kump & Barley, 2007; Mills et al., 2014), and potentially even prebiotic chemistry (e.g., Bada & Korenaga, 2018). Continents are also our best windows into the tectonic processes operating on the early Earth, preserving rocks to ~4.0 Ga (Bowring et al., 1989) and zircons even older (Wilde et al., 2001). Determining what processes created continental crust in the Hadean and Archean can help constrain when plate tectonics started (e.g., Cawood et al., 2018; Palin et al., 2020).

The predominant felsic rocks in Earth's early continents are the TTG suite (Trondhjemite-Tonalite-Granodiorites), which form by melting hydrated, mafic protocrust at ~1-2 GPa (Moyen, 2011; Moyen & Martin, 2012; Palin et al., 2016), ~35-70 km depth assuming a crustal density of 2900 $kg \cdot m^{-3}$. Several mechanisms have been proposed for the generation of TTGs. Subduction-based models appeal to elevated subducting crustal geotherms with a hotter mantle on the early Earth, such that sinking crust can melt in the P-T range for TTG genesis (Foley et al., 2002; Rapp et al., 2003). Secular cooling of the mantle then shuts off slab melting, as TTGs are rare after ~2.5 Ga (Moyen & Martin, 2012; Liu et al., 2020). Non-subduction models appeal to internal melting and differentiation of a thick, mafic crustal plateau. In such models hydrated crust at the surface is transported by volcanic burial or crustal foundering to depths where it melts to produce TTGs (e.g., Bédard, 2006; Sizova et al., 2015; Rozel et al., 2017).

Determining which TTG formation models are viable is critical for constraining the tectonic processes operating on the early Earth. Previous geodynamic studies found that slabs sank steeply and quickly at the low mantle viscosities expected for Archean temperatures (van Hunen & van den Berg, 2008). As a result, downgoing crust actually followed a colder geotherm than subducting crust today, preventing melting and potentially invalidating subduction models for TTG genesis (Perchuk et al., 2019). However, prior work assumed a modern style of subduction, with weak plate boundaries that provide negligible resistance to slab sinking.

Modeling using grain size reduction to dynamically generate plate boundaries instead finds they are relatively strong at early Earth conditions, and act to slow sinking plates (Foley, 2018; 2020). The result is a "sluggish subduction" tectonic style, where subduction is still active but slowed by resistance from the plate boundary (Foley, 2020). With slower subduction speeds, downgoing crust may heat up enough to melt at early Earth mantle temperatures, a scenario I test here.

2. Methods

I employ a simple model for the evolving temperature profile across a slab of thickness δ and the surrounding mantle extending >250km on either side of the slab. The slab sinks vertically at a speed W beneath an overriding plate with thickness δ_{op} (Fig. 1; see Supplementary Material for detailed explanation and tests of key model assumptions including a vertical slab dip angle). Slab temperature initially follows an error function profile, then evolves by heat conduction from the surrounding mantle during model evolution. The model side boundaries are fixed to the mantle temperature T_i, except for depths shallower than the base of the overriding plate, where slab top temperature is set by the parameterization from Molnar & England (1995).

Both sluggish subduction and modern-style subduction regimes are considered. In the sluggish regime the sinking speed is (Foley, 2020)

$$W = \frac{\rho g \alpha (T_{\mathrm{i}} - T_{\mathrm{n}}) L \delta}{C \mu_{\mathrm{man}} (L/d) + 2\mu_{\mathrm{sz}}} \quad (1)$$

where ρ is density, g is gravity, α is thermal expansivity, T_n is the temperature in the slab interior during subduction, L is slab length which grows as subduction proceeds, μ_{man} is mantle interior viscosity (itself a function of T_i through an Arrhenius temperature-dependent viscosity), d is the thickness of the mantle, μ_{sz} is the lithospheric shear zone viscosity, and C is a constant. The shear zone viscosity, based on application of the grain-damage theory for grain size evolution (Bercovici & Ricard, 2012), is (Foley, 2020)

$$\mu_{sz} = \mu_l^{\,p/p-m} \left(\frac{\gamma h_l A_{ref}^p}{f(\rho g \alpha (T_i - T_n) L)^2}\right)^{m/p-m} \quad (2)$$

where γ is surface tension, h_l is the grain-growth rate in the lithosphere, A_{ref} is the reference fineness (or inverse grain size) taken as 1mm, μ_l is the viscosity of the lithosphere at the reference fineness, f is the fraction of deformational work that partitions into surface energy, thereby reducing grain size, and m=2 and p=4 are constants describing the grain size dependence of viscosity (Hirth & Kohlstedt, 2003) and grain growth rate (Bercovici & Ricard, 2012), respectively. The depth, z, of the modeled slab transect deepens during subduction as

$$z = \int_0^t W(t)dt \quad (3)$$

where t is the elapsed time.

The time evolution of slab temperature profile, sinking speed, and depth are solved for as described in the supplemental material, for models covering ranges of T_i, δ, and δ_{op} as free parameters. While a range of plate thicknesses are possible in a convecting mantle at any given time, over long timescales (e.g. greater than the mantle overturn time), average plate thickness will tend towards an expected value dictated by thermal diffusion, as plates grow by thermal diffusion from ridge to trench. This expected plate thickness is:

$$\delta_{ex} \approx 2.3\sqrt{\kappa \frac{Y}{W}} \quad (4)$$

where κ is thermal diffusivity and Y=10^4km is the length of plates from ridge to trench. For each model, δ_{ex} is calculated based on the resulting average sinking speed, to check if plate thickness assumed in the model is consistent with expectations from thermal diffusion.

3. Results

At an elevated mantle temperature of T_i = 1600°C, applicable to the Archean Earth (Herzberg et al., 2010), sluggish subduction leads to melting of sinking crust while modern-style subduction does not (Figure 2). At this mantle temperature a 40km thick slab sinks rapidly, $W \approx 100$cm·yr^{-1}, for modern-style subduction, and therefore has minimal time to heat as it descends (Figures 2B & C). In the sluggish subduction regime, though, the slab initially only sinks at a speed of ≈ 1cm·yr^{-1}, speeding up to ≈ 40cm·yr^{-1} when slab length reaches ≈ 1500km. The slab then has more time to heat and slab top temperatures cross the solidus at ≈ 40km depth (Figure 2A & C). This depth of melting is also strongly controlled by the overriding plate thickness, as in either subduction style the slab top does not experience significant heating until it sinks deep enough to meet the hot mantle wedge. A thicker overriding plate therefore forces melting deeper, while a thinner overriding plate allows for shallower melting.

Models were run systematically over a range of mantle temperatures and subducting plate thicknesses with $\delta = \delta_{op}$, to map where and at what depth melting can occur for the two cases (Figure 3). A damage fraction of f=10^{-3} is used, as this produces plate speeds at z = 2000km that are $\approx 95\%$ of the modern-day Earth subduction speed, for a 100km thick slab and 1350°C mantle temperature (Figure 2D). Sluggish subduction allows for crustal melting over a wider range of mantle temperatures and subducting plate thicknesses than modern-style subduction (Figure 3). Melting between 35-70km depth, necessary for TTG genesis, is possible for $\delta \approx 35-45$km across the tested range of T_i with sluggish subduction, but only possible for a much smaller band of δ at T_i<1600°C for modern-style subduction. Increasing mantle temperature hampers slab melting for modern-style subduction (Figure 3B), because reduced viscous resistance from the mantle interior increases subduction speeds, such that downgoing crust follows a cooler geotherm for a given plate thickness as in Perchuk et al. (2019). Crustal melting then requires very thin subducting plates that sink slower and heat more rapidly. However, with sluggish subduction, plate speed only weakly increases with mantle temperature, being more strongly controlled by plate thickness, because most resistance to slab sinking is provided by the lithospheric shear zone rather than the mantle interior; high mantle temperatures then promote slab melting.

The conditions allowing for slab melting are then compared to the range of expected subducting plate thicknesses, defined as the region where δ_{ex} (from Eq. 4) and model input plate thickness match to within +/- 50% (Figure 3), the variability seen in fully dynamic convection models (Foley, 2020). For TTG genesis to be likely to occur in practice, sinking crust must melt between 35-70km depth for plate thicknesses within this δ_{ex} range. For both subduction regimes, the δ_{ex} range decreases towards thinner plates as mantle temperature increases because of a corresponding increase in average subduction speeds, which is more pronounced for modern-style subduction.

For sluggish subduction, TTG genesis becomes likely when T_i > 1620ºC and $\delta \approx 45$km, expanding to $\delta \approx 35 - 45$km for T_i = 1800ºC. At T_i < 1620ºC, though, TTG production is unlikely, as subducting slabs would have to be anomalously thin for crustal melting, like subduction of young plates on the modern Earth (Moyen & Martin, 2012). Sluggish subduction then provides a mechanism for melting downgoing crust in the hotter mantle environment of the early Earth that naturally shuts off as the mantle cools. For modern-style subduction, though, there is no overlap between the 35-70km melting depth region and the δ_{ex} range (Figure 3B), meaning TTG production is always unlikely.

The same general results hold when varying two other key model parameters for sluggish subduction, the damage partitioning fraction, f, and the overriding plate thickness, δ_{op} (Figure 4). The regions of δ-T_i space enclosed within black contour lines in Figure 4 denote where TTG genesis by slab melting is likely, as defined above. Although this TTG genesis region shifts in δ

as f is varied, it still exists at similar sizes for a wide range of f, indicating results are robust to variations in this poorly constrained parameter (Figure 4A). The baseline value of $f = 10^{-3}$, that matches present day Earth plate speeds, optimizes the likely TTG genesis region at the previously reported values of $\delta \approx 35 - 45$km and $T_i >\approx 1620$ºC.

Thinner overriding plates promote slab melting (Figures 4B) by sluggish subduction because subducting crust meets the hot mantle interior at a shallower depth, hastening crustal heating. For $\delta_{op} \approx 20 - 30$km, slab melting occurs as low as ≈ 1550°C. Meanwhile it is very difficult to induce slab melting at depths shallower than δ_{op}, so TTG generation requires $\delta_{op} \leq 50 - 60$km, similar to the required subducting plate thicknesses. Absent a reason to expect overriding plates to be significantly thinner than subducting plates, results indicate the previously listed ranges of δ and T_i as optimal for TTG genesis.

4. Discussion

A sluggish subduction regime operating on the early Earth allows for subducting crust to melt and produce TTGs when the mantle temperature is >1600ºC and subducting and overriding plates are $\approx 35 - 45$km thick. Meanwhile, TTGs cannot be generated by slab melting with modern-style subduction: slabs sink too quickly in a hotter mantle for crustal melting, consistent with previous studies (van Hunen & van den Berg, 2008; Bouilhol et al., 2015; Perchuk et al., 2019). This finding provides further evidence that the dominant force balance in modern subduction zones, between plate buoyancy and viscous resistance from the mantle interior, may not apply to the early Earth. Plates moving as fast as the modern-style force balance predicts are also not consistent with paleomagnetic constraints (Swanson-Hysell, 2021) or Earth's thermal evolution (Korenaga, 2006). The effects of lithospheric grain size reduction naturally produce the sluggish subduction style that allows TTG genesis by slab melting at high mantle temperatures, as the viscous resistance to slab sinking by lithospheric shear zones becomes more important as mantle temperature increases with this mechanism (Foley, 2018; 2020). However, that slow plates promote slab melting to form TTGs is a general result of the modeling and applies regardless of the underlying rheological mechanism for this behavior (see also Capitanio et al., 2019).

That crustal melting during sluggish subduction is only feasible at high mantle temperatures also naturally explains the prominence of TTGs in the Archean and their paucity post 2.5 Ga. Herzberg et al. (2010) estimate mantle temperatures peaked at $T_\mathrm{i} \gtrsim 1600$°C in the Archean, cooling below this by 2.5 Ga or soon after; with this temperature evolution sluggish subduction produces TTGs exclusively in the Hadean and Archean. As the mantle cools at the end of the Archean, typical plates then become too thick for crustal melting. TTG genesis becomes increasingly rare, confined to subduction of very young, thin plates. This same general explanation for the age distribution of TTG genesis also holds for different mantle temperature history estimates (Supplemental Material).

Even at high mantle temperatures, slab melting during sluggish subduction requires plates at the low end of the expected plate thickness range, meaning it could be limited in both space and time. Slow subduction of thinner than average lithosphere is seen after major overturn events in dynamic convection models (Foley, 2020); these might be prime periods for TTG production by slab melting. As a result, other mechanisms, such as plateau melting (e.g., Bédard, 2006; Rozel et al., 2017; Bauer et al., 2020), may have also been important and active at the same time (e.g., Van Kranendonk, 2010). Slow plates in fact could promote crustal plateau formation by keeping some regions above hot mantle upwellings for extended periods. Sluggish subduction may have acted in concert with plateau melting to produce early Earth TTGs, demonstrating that multiple, complementary pathways exist for creating Earth's earliest continents.

ACKNOWLEDGMENTS

This work was supported by NSF awards EAR-1723057 and EAR-2046598. I thank Jeroen van Hunen, Andy Smye, and Jesse Reimink for discussions during the development of this paper, and helpful reviews by Richard Palin, Fabio Capitanio, and an anonymous reviewer.

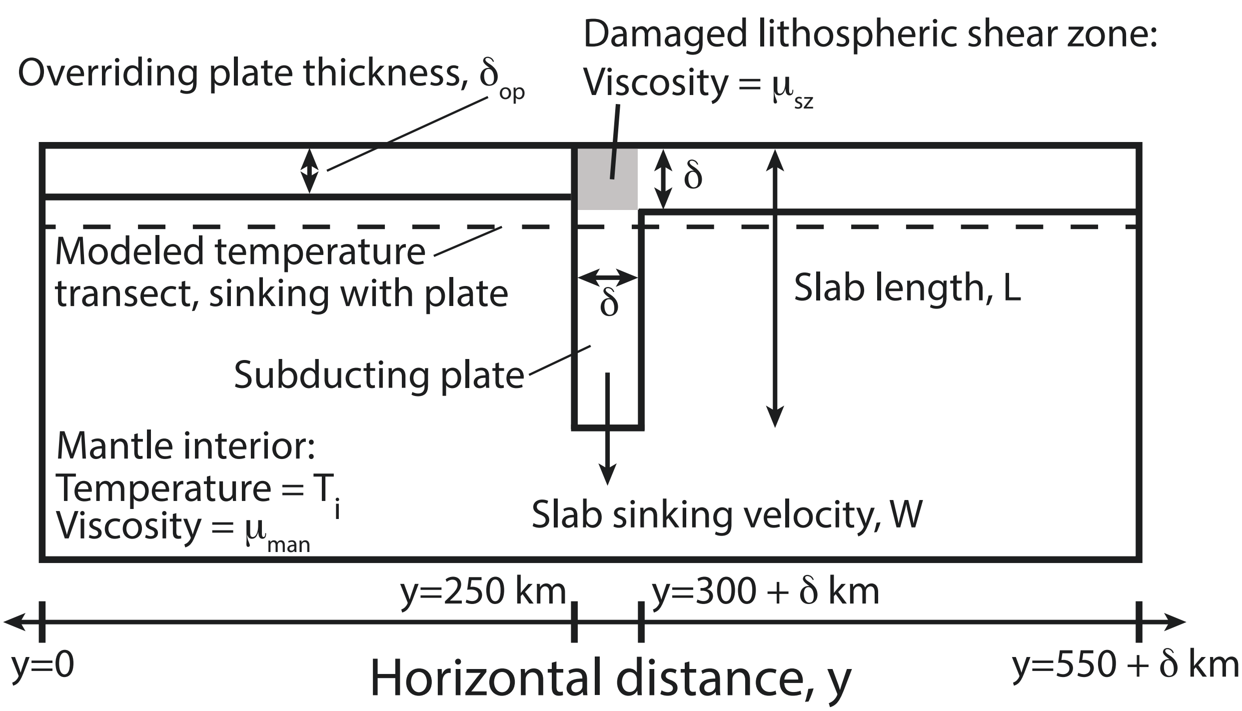

Figure 1. Sketch of the model setup. Temperature is calculated along a transect through the plate and surrounding mantle (dashed line), moving with the subducting plate.

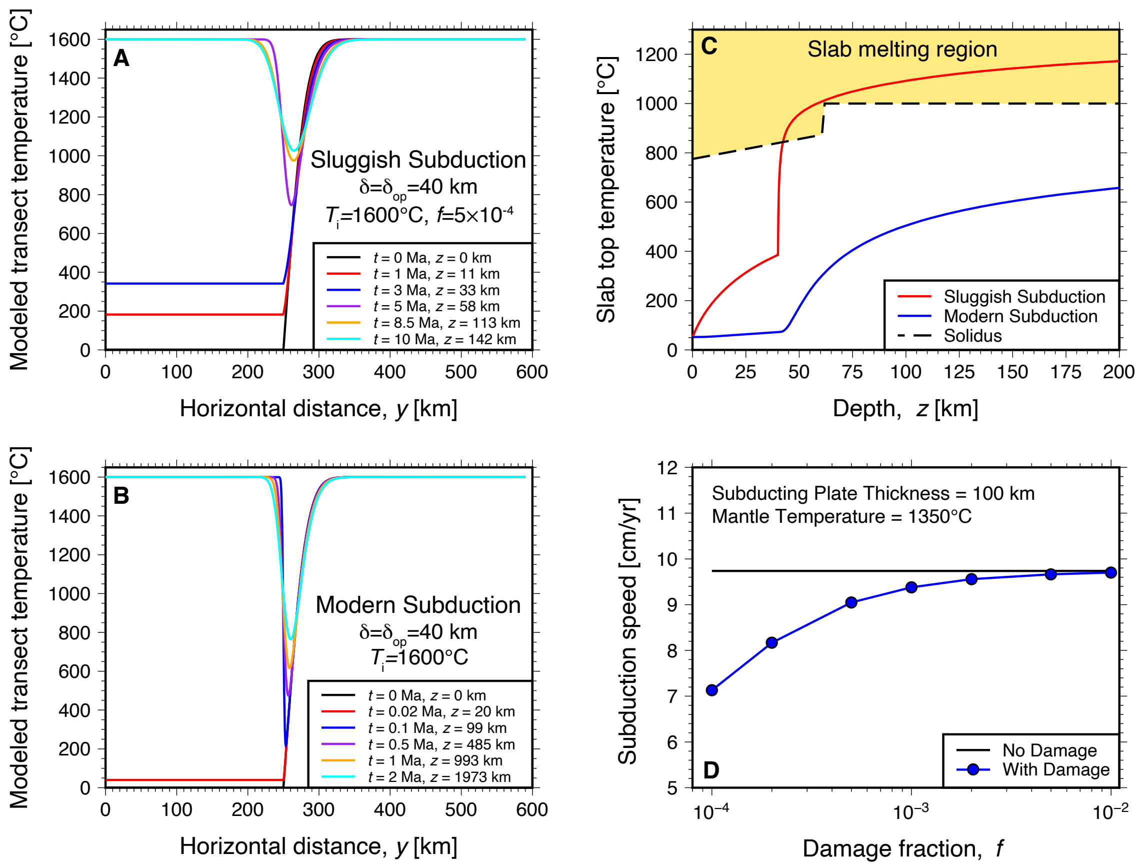

Figure 2. Temperature transects through the slab and surrounding mantle or overriding plate, depending on depth, z, for sluggish subduction (A) and modern-style subduction (B). Transects are shown at different times, t, which correspond to different depths based on the subduction speed (see legend). Slab top temperature as a function of depth for the same models of modern-style and sluggish subduction (C); dashed line shows the solidus for the subducting slab. Models use $\delta = \delta_{op} = 40$km and $T_i = 1600$°C, and $f = 5\times10^{-4}$ for sluggish subduction. D) Subduction speed reached by a depth of 2000 km for models with an Earth-like subducting plate thickness of δ=100km and mantle temperature of $T_i = 1350$°C as a function of the fraction of deformational work partitioning into grain-damage, f. The modern-style subduction sinking speed of ≈ 10cm·yr^{-1} for these conditions is shown as a solid black line.

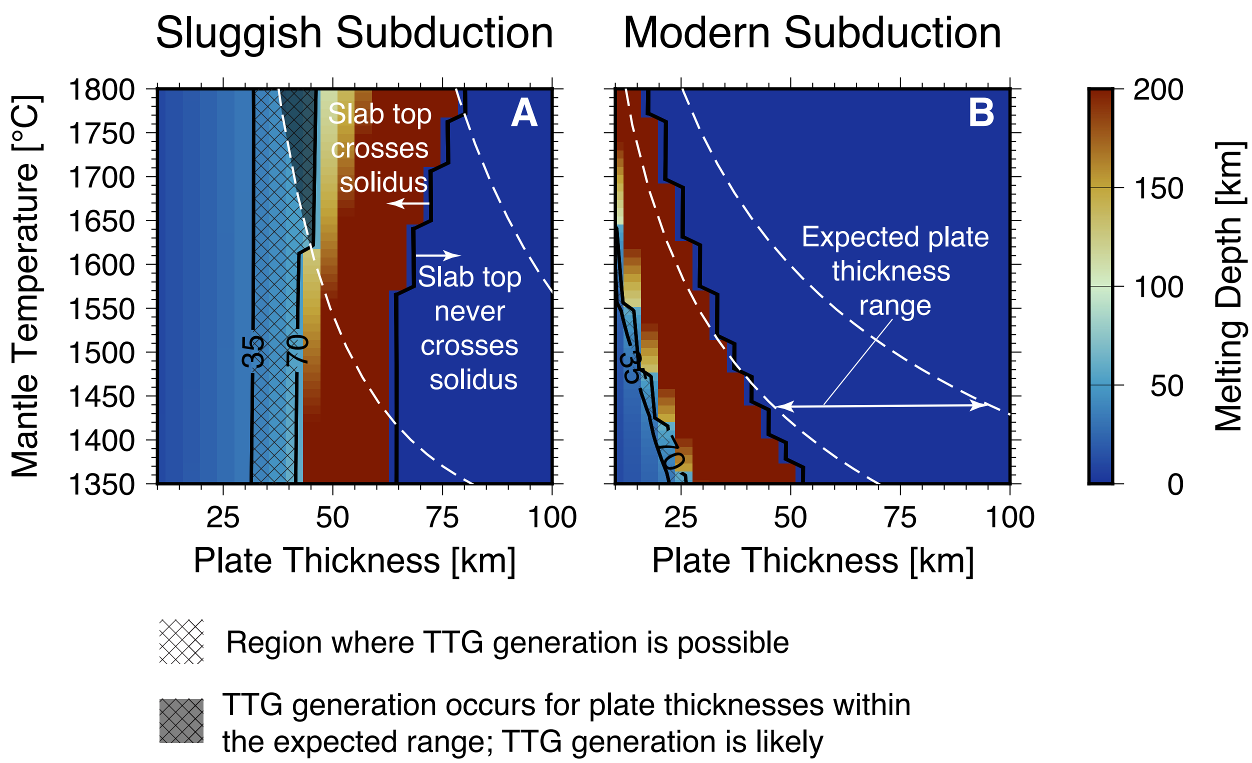

Figure 3. Depth of crustal melting for sluggish subduction (A) and modern-style subduction (B) as a function of subducting plate thickness and mantle temperature; melting depth of 0km indicates sinking crust never crosses the solidus. Hashed region marks where crustal melting is possible in the 35-70 km depth range needed for TTG genesis; shaded hashed region shows where this occurs for subducting plate thicknesses within the expected range (denoted by dashed white lines), and hence where TTG production is likely to occur in practice. The range of expected lithosphere thicknesses assumes +/- 50% variation around the calculated value of δ_{ex}. For all models $\delta = \delta_{op}$ and for the sluggish subduction models f=10^{-3}.

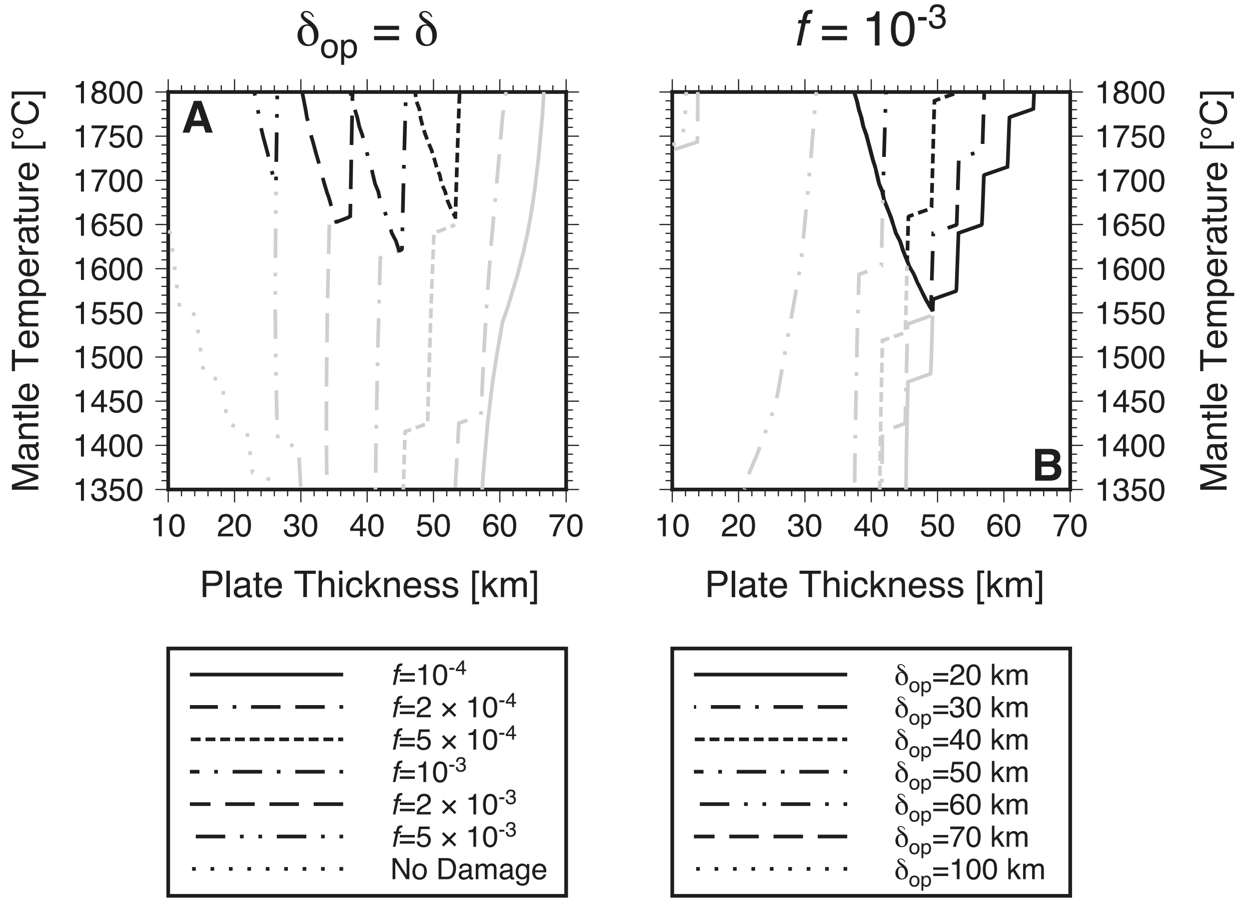

Figure 4. Contour lines marking where subducting crust melts at 70 km depth, the maximum for generating TTGs, as a function of subducting plate thickness and mantle temperature, along with the lower bound on expected plate thickness, shown only when the 70 km melt depth contour falls within the δ_{ex} range (i.e. when the lower bound on δ_{ex} is to the left of the contour line). The 70 km melt depth contour is colored gray when it does not fall within the expected plate thickness range, and black when it does. Black lines then enclose the range of subducting plate thicknesses where TTG production is likely. A) Damage fraction, f, is varied with $\delta = \delta_{op}$ ("no damage" case corresponds to modern-style subduction) and B) δ_{op} is varied with fixed f (note that the δ_{ex} lower bounds are the same for all δ_{op} and plot on top of each other).

REFERENCES CITED

Bada, J., and Korenaga, J., 2018, Exposed areas above sea level on Earth >3.5 Gyr ago: Implications for prebiotic and primitive biotic chemistry: Life, v. 8(4), p. 55, doi:10.3390/life8040055.

Bauer, A., Reimink, J., Chacko, T., Foley, B., Shirey, S., and Pearson, D., 2020, Hafnium isotopes in zircons document the gradual onset of mobile-lid tectonics: Geochem. Perspect. Lett., v. 14, p. 1–6.

Bédard, J.H., 2006, A catalytic delamination-driven model for coupled genesis of Archaean crust and sub-continental lithospheric mantle: Geochim. Cosmochim. Acta, v. 70, p. 1188-1214, doi:10.1016/j.gca.2005.11.008.

Bercovici, D., and Ricard, Y., 2012., Mechanisms for the generation of plate tectonics by two-phase grain-damage and pinning: Phys. Earth Planet. Inter., v. 202, p. 27-55, doi:10.1016/j.pepi.2012.05.003.

Berner, R.A., Lasaga, A.C., and Garrels, R.M., 1983, The carbonate-silicate geochemical cycle and its effect on atmospheric carbon dioxide over the past 100 million years: Am. J. Sci., v. 283(7), p. 641–683.

Bouilhol, P., Magni, V., van Hunen, J., and Kaislaniemi, L., 2015, A numerical approach to melting in warm subduction zones: Earth and Planetary Science Letters, v. 411, p. 37-44, doi:10.1016/j.epsl.2014.11.043.

Bowring, S. A., Williams, I. S., & Compston, W. 1989. 3.96 Ga gneisses from the Slave province, Northwest Territories, Canada. Geology, 17 (11), 971. doi:10.1130/0091-7613(1989)017(0971:GGFTSP)2.3.CO;2.

Capitanio, F.A., Nebel, O., Cawood, P.A., Weinberg, R.F., and Chowdhury, P., 2019, Reconciling thermal regimes and tectonics of the early Earth: Geology, v. 47(10), p. 923-927, doi:10.1130/G46239.1.

Cawood, P.A., Hawkesworth, C.J., Pisarevsky, S.A., Dhuime, B., Capitanio, F.A., and Nebel, O., 2018, Geological archive of the onset of plate tectonics: Philos. Trans. Royal Soc. A, v. 376, p. 2132, 20170405. doi:10.1098/rsta.2017.0405.

Flament, N., Coltice, N., and Rey, P. F., 2008, A case for late-Archaean continental emergence from thermal evolution models and hypsometry: Earth Plane. Sci. Lett., v. 275(3-4), p. 326-336, doi:10.1016/j.epsl.2008.08.029.

Foley, B.J., 2018, The dependence of planetary tectonics on mantle thermal state: applications to early Earth evolution: Philos. Trans. Royal Soc. A, v. 376, p. 20170409, doi:10.1098/rsta.2017.0409.

Foley, B.J., 2020, Timescale of short-term subduction episodicity in convection models with grain damage: Applications to Archean tectonics: J. Geophys. Res. Solid Earth, v. 125(12), p. e20478, doi:10.1029/2020JB020478.

Foley, S., Tiepolo, M., and Vannucci, R., 2002, Growth of early continental crust controlled by melting of amphibolite in subduction zones: Nature, v. 417, p. 837-840, doi:10.1038/nature00799.

Hayworth, B.P.C., and Foley, B.J., 2020, Waterworlds may have better climate buffering capacities than their continental counterparts: Astrophys. J. Lett., v. 902(1), p. L10, doi:10.3847/2041-8213/abb882.

Hirth, G., Kohlstedt, D., 2003, Rheology of the upper mantle and the mantle wedge: a view from the experimentalists, *in* J. Eiler, ed., Subduction factory monograph, v. 138: Am. Geophys. Union, Washington, DC, p. 83-105.

Hofmann, A.W., 1988, Chemical differentiation of the Earth: the relationship between mantle, continental crust, and oceanic crust: Earth and Planetary Science Letters, v. 90(3), p. 297-314, doi:10.1016/0012-821X(88)90132-X.

Korenaga, J. 2006. Archean geodynamics and the thermal evolution of Earth, *in* K. Benn, J.-C. Mareschal, K. Condie, eds, Archean Geodynamics and Environments, v. 164: Am. Geophys. Union, Washington, DC, p. 7-32.

Kump, L.R., and Barley, M.E., 2007, Increased subaerial volcanism and the rise of atmospheric oxygen 2.5 billion years ago: Nature, v. 448(7157), p. 1033-1036, doi:10.1038/nature06058.

Liu, H., Sun, W.-d., and Deng, J.-H., 2020, Transition of subduction-related magmatism from slab melting to dehydration at 2.5 Ga: Precambrian Research, v. 337, p. 105524, doi:10.1016/j.precamres.2019.105524.

Mills, B., Lenton, T.M., Watson, A.J., 2014, Proterozoic oxygen rise linked to shifting balance between seafloor and terrestrial weathering: Proc. Natl. Acad. Sci., v. 111, p. 9073-9078, doi:10.1073/pnas.1321679111.

Molnar, P., England, P., 1995, Temperatures in zones of steady-state underthrusting of young oceanic lithosphere: Earth Planet. Sci. Lett., v. 131(1), p. 57-70, doi:10.1016/0012-821X(94)00253-U.

Moyen, J.-F., 2011, The composite Archaean grey gneisses: Petrological significance, and evidence for a non-unique tectonic setting for Archaean crustal growth: Lithos, v. 123(1), p. 21-36, doi:10.1016/j.lithos.2010.09.015.

Moyen, J.-F., and Martin, H., 2012, Forty years of TTG research: Lithos, v. 148, p. 312– 336.

Palin, R.M., White, R.W. and Green, E.C., 2016, Partial melting of metabasic rocks and the generation of tonalitic–trondhjemitic–granodioritic (TTG) crust in the Archaean: Constraints from phase equilibrium modelling: Precambrian Research, v. 287, p. 73-90.

Palin, R.M., Santosh, M., Cao, W., Li, S.S., Hernández-Uribe, D. and Parsons, A., 2020, Secular change and the onset of plate tectonics on Earth: Earth-Science Reviews, v. 207, p. 103172.

Perchuk, A.L., Zakharov, V.S., Gerya, T.V., and Brown, M., 2019, Hotter mantle but colder subduction in the Precambrian: What are the implications?: Precambrian Res., v. 330, p. 20-34, doi:10.1016/j.precamres.2019.04.023.

Rapp, R.P., Shimizu, N. and Norman, M.D., 2003, Growth of early continental crust by partial melting of eclogite: Nature, v. 425(6958), p. 605-609.

Reimink, J.R., Davies, J.H.F.L., and Ielpi, A., 2021, Global zircon analysis records a gradual rise of continental crust throughout the Neoarchean: Earth and Planetary Science Letters, v. 554, p. 116654, doi:10.1016/j.epsl.2020.116654.

Rozel, A.B., Golabek, G.J., Jain, C., Tackley, P.J., and Gerya, T., 2017, Continental crust formation on early Earth controlled by intrusive magmatism: Nature, v. 545, p. 332-335, doi:10.1038/nature22042.

Rudnick, R.L., and Gao, S., 2014, 4.1 - Composition of the continental crust, *in*, R.L. Rudnick, K.K. Turekian, and H.D. Holland, eds., Treatise on geochemistry (second edition) Vol. 4: Elsevier, Oxford, p. 1-51, doi:10.1016/B978-0-08-095975-7.00301-6.

Sizova, E., Gerya, T., Stüwe, K. and Brown, M., 2015, Generation of felsic crust in the Archean: a geodynamic modeling perspective: Precambrian Research, v. 271, p. 198-224.

Swanson-Hysell, N. L., 2021, The Precambrian paleogeography of Laurentia, *in* L. Pesonen, J. Salminen, S.-Å. Elming., D. Evans, and T. Veikkolainen, eds., Ancient supercontinents and the paleogeography of Earth: Elsevier, Oxford, p. 109-153.

van Hunen, J., van den Berg, A.P., 2008, Plate tectonics on the early Earth: Limitations imposed by strength and buoyancy of subducted lithosphere: Lithos, v. 103, p. 217-235, doi:10.1016/j.lithos.2007.09.016.

Van Kranendonk, M.J., 2010, Two types of Archean continental crust: Plume and plate tectonics on early Earth: Am. J. Sci., v. 310(10), p. 1187-1209.

Wilde, S.A., Valley, J.W., Peck, W.H., and Graham, C.M., 2001, Evidence from detrital zircons for the existence of continental crust and oceans on the Earth 4.4 Gyr ago: Nature, p. 409, v. 175-178, doi:10.1038/35051550.

[1]Supplemental Material. Extended description of the methods and benchmark comparisons to two-dimensional dynamic subduction models are provided. Further robustness tests of the main results to assumptions in the model setup are also shown. Please visit https://doi.org/10.1130/XXXX to access the supplemental material, and contact editing@geosociety.org with any questions.